Supporting Information

Electrochemical Water Oxidation Reaction by Dinuclear Re (V) Oxo Complexes with 1, 4-Benzoquinone Core via Redox Induced Electron Transfer (RIET) Process

Uday Shee [a], Debopam Sinha [a,b], Sandip Mondal [c*], Kajal Krishna Rajak[a*]

[a]*Inorganic Chemistry Section, Department of Chemistry, Jadavpur University, Kolkata, 700032, India.*
E-mail: kajalrajak@gmail.com

[b]*Department of Chemistry, Vijaygarh Jyotish Ray College, Kolkata, 700032, India*

[c]*Department of Chemistry, Darjeeling Govt. College, Darjeeling, 734101, India.*
E-mail: sandipmondal30@gmail.com

Table of Contents	Page No.
Experimental Section: Materials and Physical Measurements	S3-S5
Syntheses	S5
IR spectra of **1** and **2**	S6
^{1}H NMR spectra of the complex **1**in CD_3CN	S6
^{13}C NMR spectra of the complex**1** and Complex **2**in CD_3CN	S7
ESI-MS of intermediate of **A**^{1}	S8
FT-IR spectrum of Complex **1** before and after bulk electrolysis in CH_3CN/Water mixture at 1.3 V	S9
ESI-MS of intermediate of **A**^{2}	S9
Water oxidation in Homogeneous Medium: H_2O concentration dependence analysis of the complexes **1** and **2**	S10
Water oxidation in Homogeneous Medium: Catalyst concentration dependence analysis of the complexes **1** and **2**	S11
Calculation of diffusion constants from cyclic voltammogram	S12
O_2 produced during OER (Oxygen Evolution Reaction) reduced in-situ by the working electrode at the reverse cathodic scan at argon atmosphere	S13
Calculation of Faradaic Yield for Complex **1**	S14
TOF$_{max}$ calculations of catalyst Complex **1** from cyclic voltammetry experiments	S14
GC-TCD graph for oxygen detection over time	S13
Amount of Oxygen determination by GC-chromatogram(Headspace analysis) and calculation of TON AND TOF.	S14
I–t curves and charge buildup during CPE	S15
Comparison the water oxidation catalytic activity of Complex **1** and Complex **2**	S15
X-ray crystallographic data of complex **1**	S15
Experimental and theoretical bond lengths of complex **1** and theoretical bond lengths of **1**$^+$ and **1**$^-$	S16
Molecular geometry of Complex **2**	S16
Isodensity plot of the selected orbital and Spin density plot of the excited states for Complex **1**	S17
Isodensity plot of the selected orbital and Spin density plot of the excited states for Complex **2**	S18
Main calculated optical transition for the complex **1** with composition in terms of molecular orbital contribution of the transition, vertical excitation energies (λ/nm), and oscillator strength in acetonitrile.	S19
References	S20-S21

Experimental Section

Experimental Details*:*

Materials:

All chemicals used in the synthesis were of reagent grade and used without further purification. 2, 5 dihydroxy 1, 4 benzoquinone (H_2DBQ) and Chloranilic acid (H_2CA) were purchased from Sigma-Aldrich. Solvents were distilled from the appropriate drying agents under nitrogen before use. All syntheses were performed in a dry oxygen-free box.

Instrumentation Details:

Electron Paramagnetic Resonance (EPR) spectrum:

EPR spectrum was taken for the sampleinstandard quartz EPR tubes using a JEOL JES-FA200 X-band spectrometer. Instrument settings: microwave frequency, 9.431 GHz; microwave power, 0.998 mW; modulation frequency, 100 kHz.

X-Ray crystallography:

The single crystals suitable for X-ray crystallographic analysis of the complexes were obtained by slow evaporation of the respective solution system. The X-ray intensity data were collected on Bruker AXS SMART APEX CCD diffractometer equipped with a Mo target rotating-anode X-ray source and a graphite mono chromator (Mo Kα, λ = 0.71073 Å) at 293 K. The data were reduced in SAINTPLUS and empirical absorption correction was applied using the SADABS package. [1] Full matrix least-square procedure on F^2 was used for structure refinement. All non-hydrogen atoms were refined anisotropically. All calculations reported in this article were performed using the SHELXTL V 6.14 program package. [2] Molecular structure plots were drawn using the ORTEP and Mercury software's. [3]

Electrochemical measurements:

All electrochemical experiments were performed using a CH Instruments Electrochemical Analyser.

Homogeneous electrochemistry:

Cyclic Voltammetry (CV) of **Complex 1** and **Complex 2** were recorded inside the glove box under inert dinitrogen atmosphere. Glassy carbon (GC), sealed aq. Ag/AgCl (saturated KCl) and Pt wire were used as working, reference and as counter electrodes respectively.

Controlled potential Electrolysis (CPE):

The CPE experiments of complexes **1** and **2** with water were performed in a standard H cell where the counter chamber and the working chamber were separated by a glass frit. In the working chamber glassy carbon electrode, sealed aq. Ag/AgCl (saturated KCl) and Pt wire were used as working, reference and as counter electrodes respectively.

Gas Detection by Gas Chromatography (GC):

The gas evolved during BE was detected by using GC instrument of model no. 8860 (G2790A), serial no. CN2211C039 fitted with TCD. 500 µl gases was syringed out by a gas tight syringe from the head space of the working chamber of the H cell and was injected into the inlet of the GC.

Computational Study:

The geometrical structure was optimized without any symmetry constraints by the DFT[4] method with non-local correlation functional of Lee–Yang–Parr (B3LYP)[5.] Calculation approach[6] associated with the effective core potential (ECP) approximation of Hay and Wadt was used for describing the $(1s^2 2s^2 2p^6)$ core electron for vanadium whereas the associated "double-ξ"quality basis set LANL2DZ was used for the valence shell[7]. For H atoms, we used 6-31+G basis set, for non-hydrogen atoms C, N and O, we employed 6-311+G basis set. All

the calculations were performed with the Gaussian 09W software package[8] supported by Gauss View 5.1 software.

Syntheses of Complexes 1 and 2

[Cl$_3$ORe(v)(DBQ^{2-})Re(v)Cl$_3$O](NBu$_4$)$_2$(1):

To a 10 ml acetone solution of [ReOCl4]$^+$[NBu4]$^-$ (60 mg, 0.1 mmol) was added to a acetone solution (10 mL) of H2DBQ (7 mg, 0.05mmol) in a wet box. Then, the solution became dark blue. After stirring about 2 hours at room temperature, the precipitation came out. This precipitation was layered in CH2Cl2 and n-hexane. Single crystals of 1 were obtained by slow diffusion of n-hexane to a CH2Cl2 solution of crude product of 1 at RT. [Yield: 40 mg (59.7% with respect to rhenium)]. 1H NMR (CD3CN, 400 MHz): δ 5.78 (s, 2H), 1.89-1.80(m,16H),1.45(h, j=7.3Hz, 16H), 1.00(t, j=7.3 Hz, 24 H); 13C NMR (CD3CN, 101MHz): δ 179.48, 174.85, 174.61, 172.82, 103.39, 59.37, 24.32, 20.33(d, j=2.5 Hz), 13.81; IR (cm−1): ν (CO): 1530, ν (Re=O): 990. Anal. calcd for C$_{38}$H$_{74}$Cl$_6$N$_2$O$_6$Re$_2$: C, 36.80; H, 6.01; N, 2.26. Found: C, 37.71; H, 6.20; N, 2.43.

[Cl$_3$ORe(V)(CA^{2-})Re(V)Cl$_3$O](NBu$_4$)$_2$ (2):

To a 10 ml acetone solution of [ReOCl4][NBu4] (60 mg, 0.1 mmol) was added a acetone solution (10 ml) of CA (10 mg, 0.05mmol) in a wet box, and the solution became dark blue. After stirring about 2 hours at room temperature, the precipitation comes out. This precipitation was layered in CH2Cl2and n-hexane mixture. Single crystals of 2 were obtained by slow diffusion of n-hexane to a CH2Cl2 solution of crude product of 2 at RT.[Yield: 45 mg (64%with respect to rhenium]. 13C NMR (CD3CN, 101 MHz): δ 172.07, 167.93, 167.59, 166.32, 107.34, 58.50-58.34(m), 23.37, 19.39 (d,j=2.3Hz), 12.86; IR (cm−1): ν (CO): 1510,ν (Re=O): 990. Anal. calcd for C$_{38}$H$_{72}$Cl$_8$N$_2$O$_6$Re$_2$: C, 34.87; H, 5.54; N, 2.14. Found: C, 35.23; H, 5.46; N, 2.28.
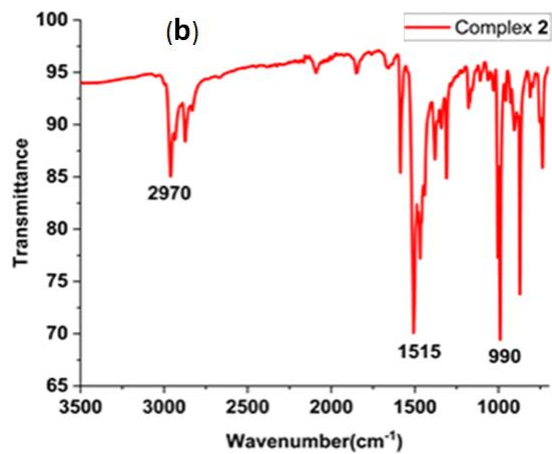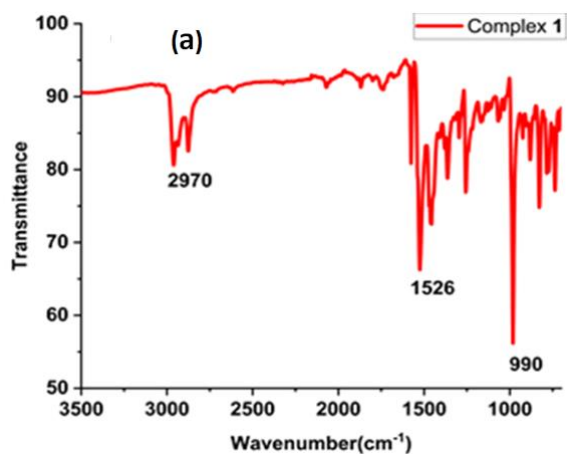
Figure S1.Infra-red spectra of (a) **1**and (b) **2**
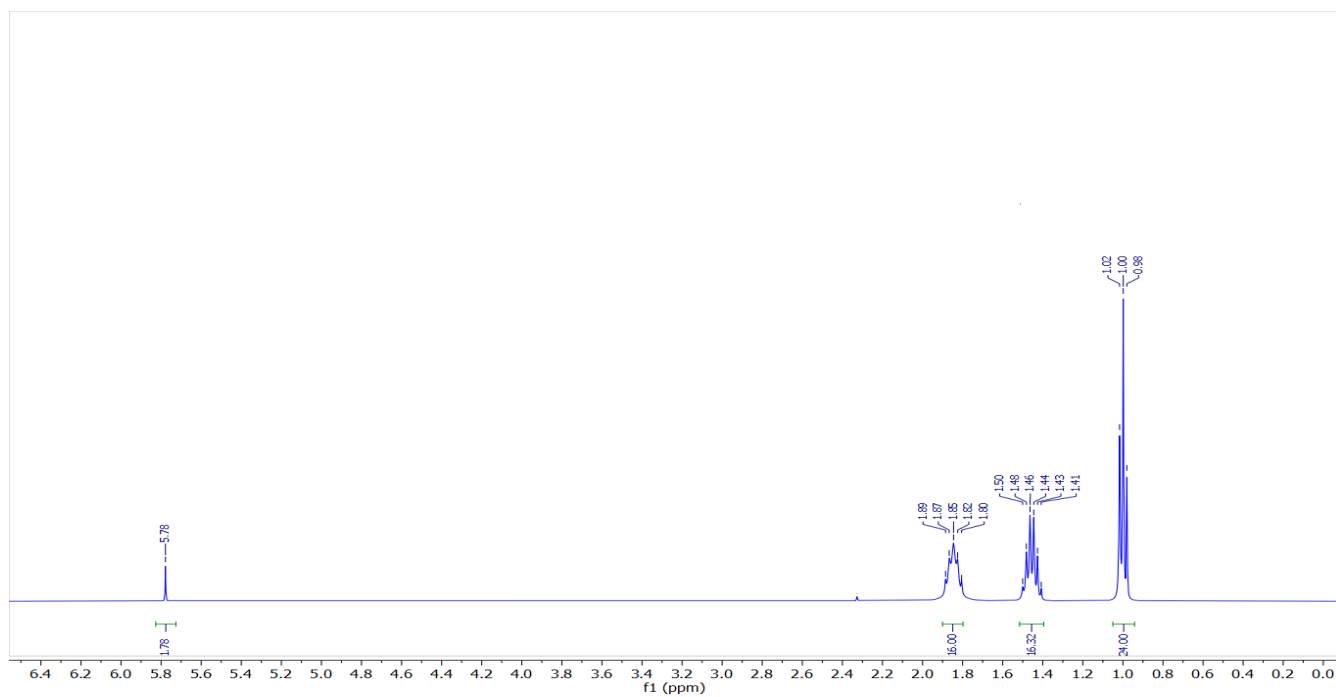

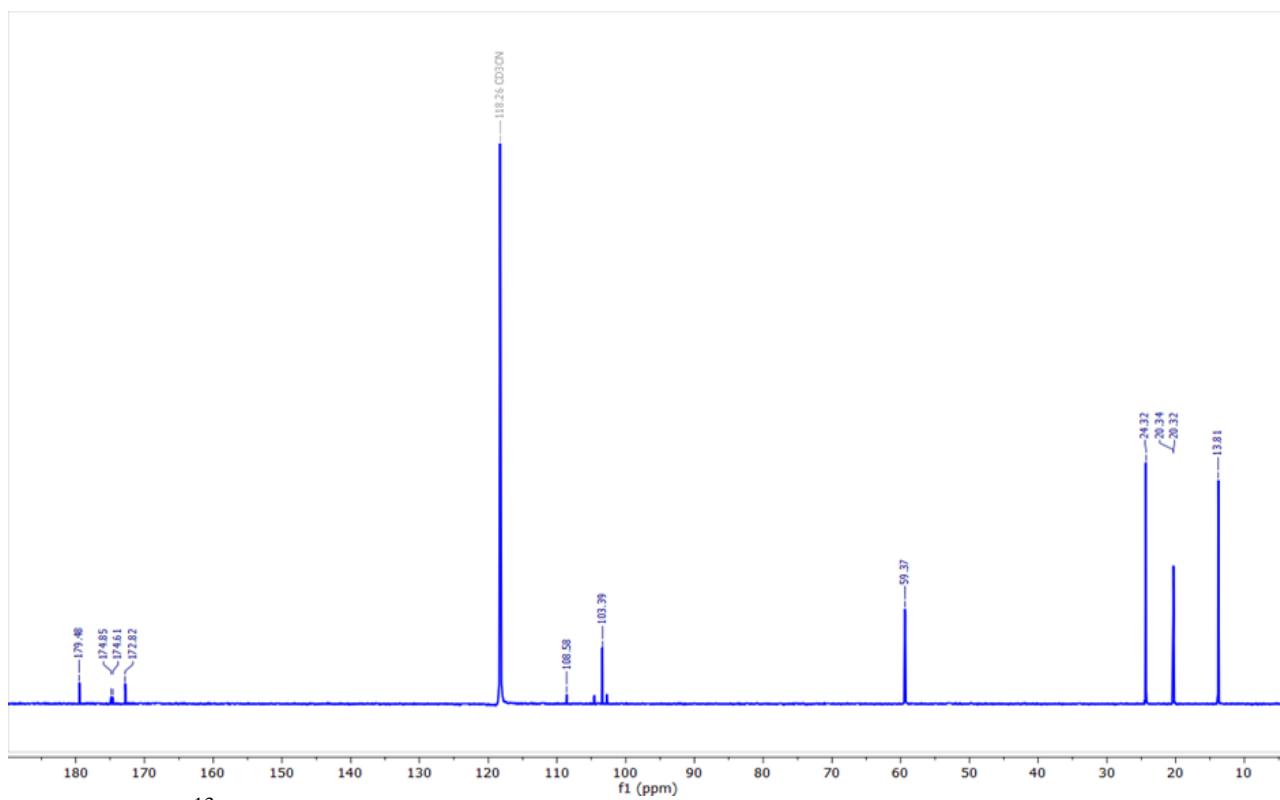**Figure S2**. ^{1}H NMR spectra of the complex **1**in CD$_3$CN

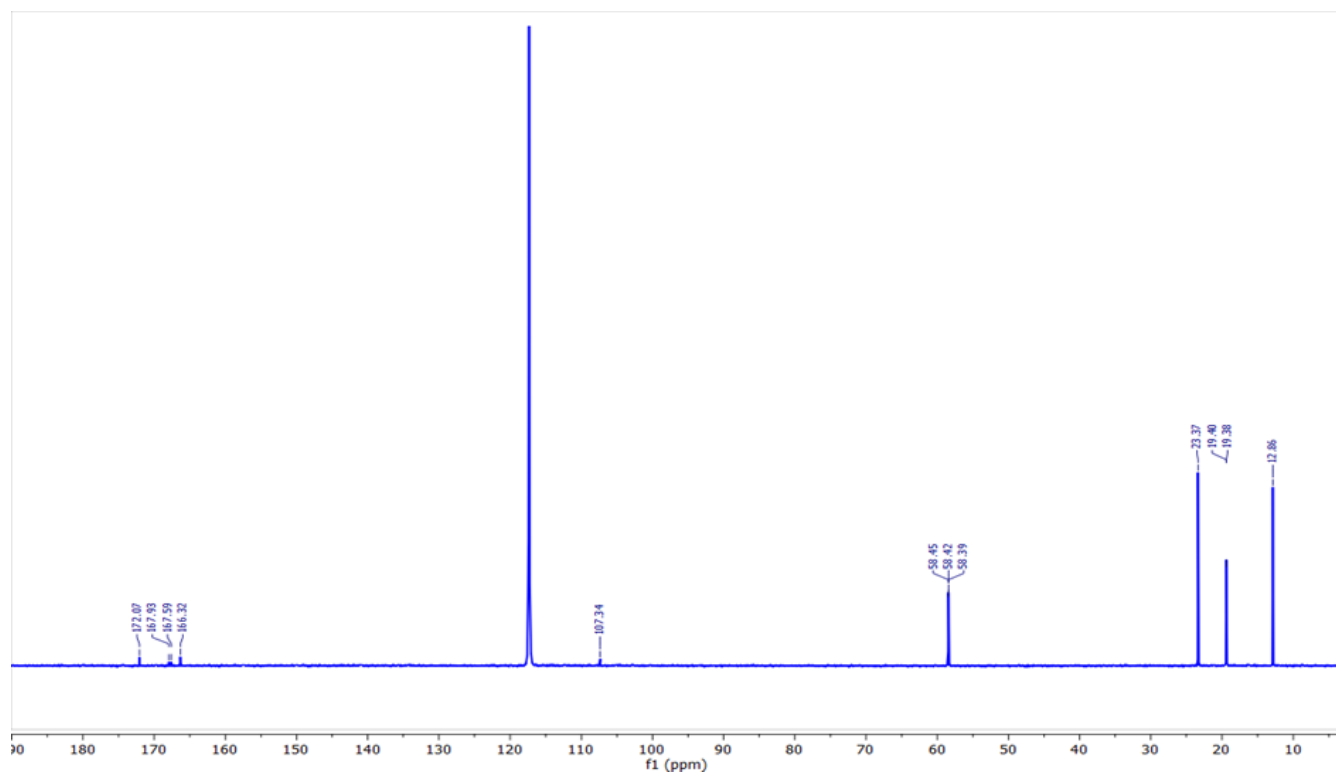**Figure S3**. ^{13}C NMR spectra of the complex **1** in CD_3CN

Figure S4. ^{13}C NMR spectra of the complex **2** in CD_3CN
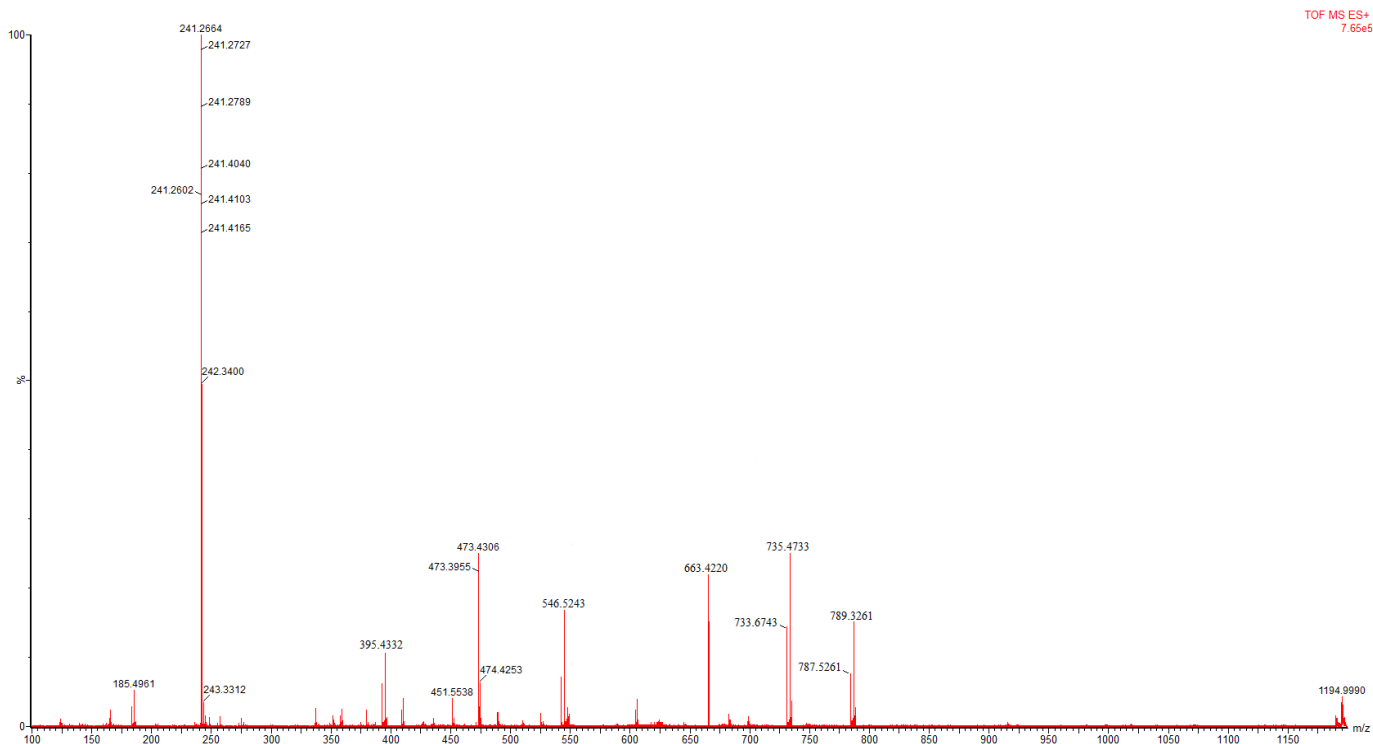
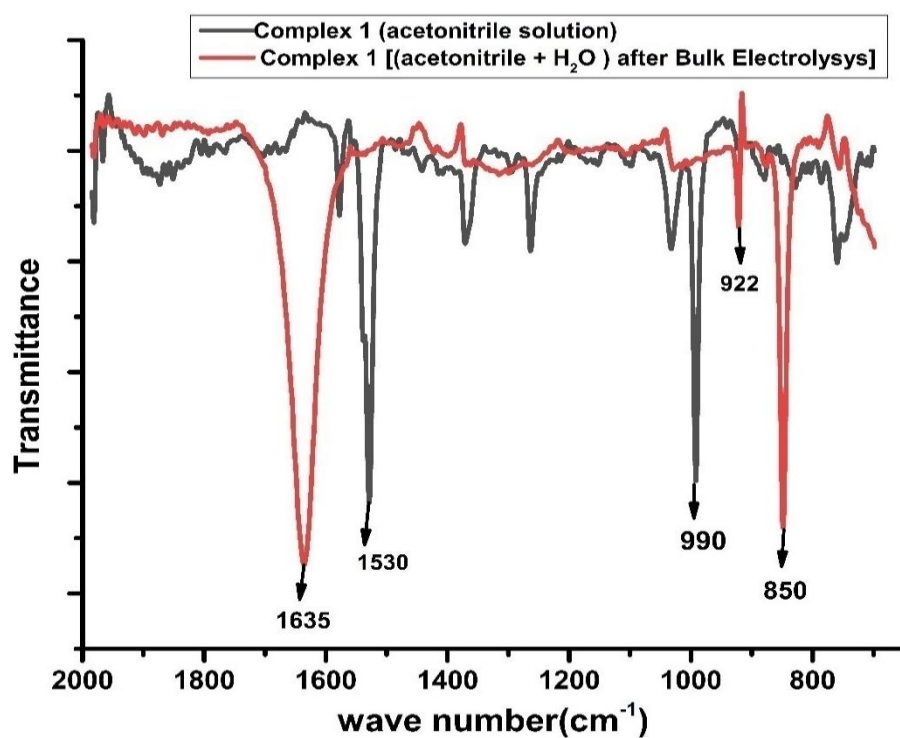**Figure S5.** ESI-MS Spectra of the Intermediate A^1 for catalysis of complex **1**

Figure S6. FT-IR spectrum of Complex **1** before and after bulk electrolysis in CH_3CN/Water mixture at 1.3 V

Water oxidation in Homogeneous Medium:

0.5 mM solution of the complex was prepared in degassed acetonitrile for electrochemical studies. Tetrabutylammonium perchlorate (TBAP) was used as supporting electrolyte. Glassy carbon (GC), sealed aq. Ag/AgCl (saturated KCl) and Pt wire were used as working, reference and as counter electrodes respectively. All CVs were collected with scan rates of 100 mV/s for the electro-catalytic water oxidation studies in acetonitrile-water mixture.
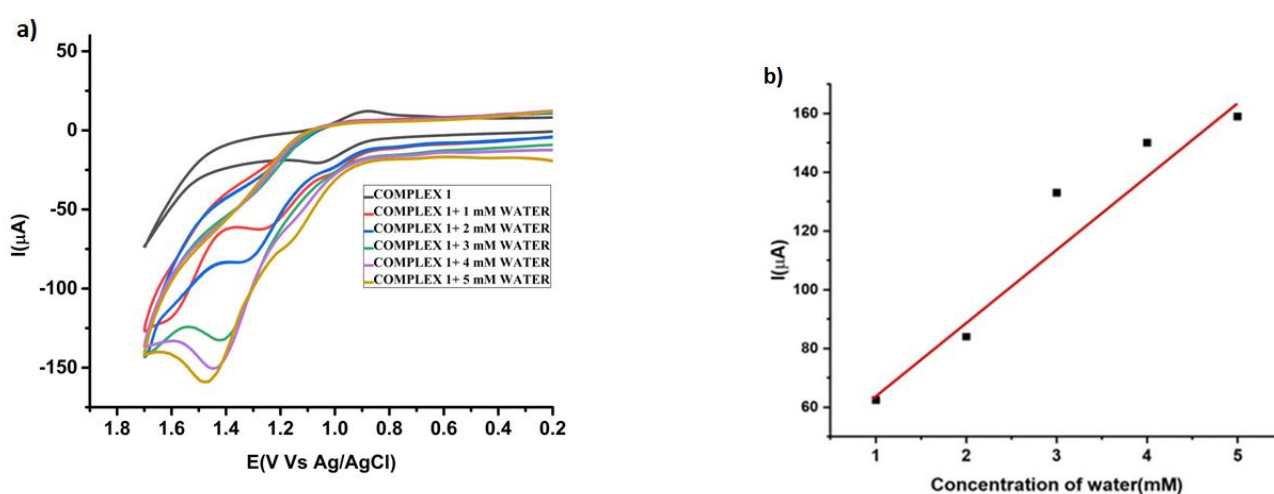
Figure S7. H_2O concentration dependence of catalysis of Complex **1** (a) Current *vs.* potential plot with gradual addition of 1μM of water and (b) Current vs. Concentration of water plo
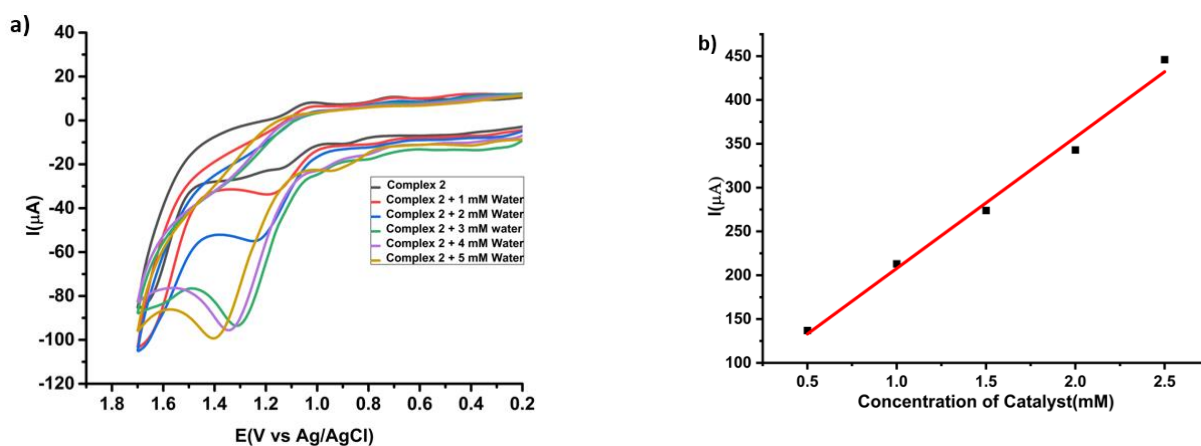
Figure S8. H_2O concentration dependence of catalysis of Complex **2** (a) Current *vs.* potential plot with gradual addition of 1μM of water and (b) Current vs. Concentration of water plot
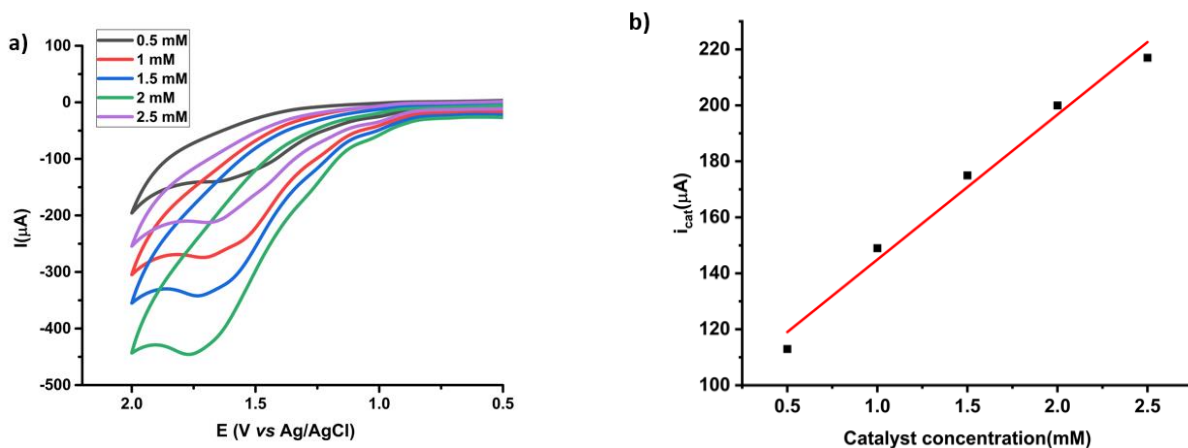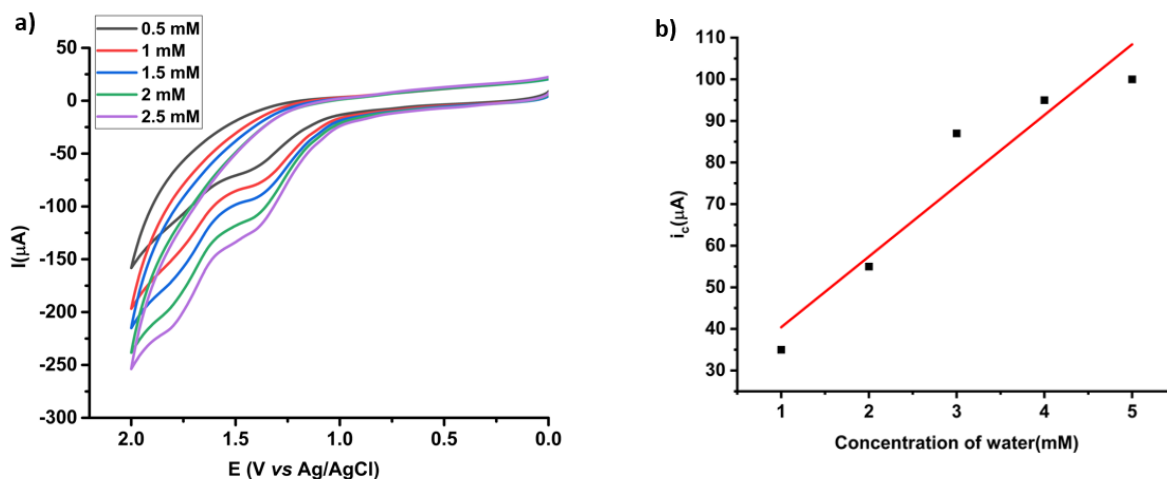
Figure S9. Catalyst concentration dependence of catalysis of Complex **1 a)** Current *vs.* potential plot with gradual addition of 0.5 μM of catalyst and **b)** Current vs. Concentration of Catalyst plot

Figure S10. Catalyst concentration dependence of catalysis of Complex **2** (a) Current *vs.* potential plot with gradual addition of 0.5 μM of catalyst and (b) Current vs. Concentration of Catalyst plot

Calculation of diffusion constants from cyclic voltammogram:

The peak current is given by the Randles-Sevcik equation (1).

$$i_P = 0.4463(F/RT)^{1/2}n_P{}^{3/2}FAD^{1/2}[C]v^{1/2} \qquad (1)$$

In equation (1), i_p is peak current, F is Faraday's constant (F = 96500 C mol^{-1}), R is the universal gas constant (R = 8.31 J K^{-1} mol^{-1}), T is temperature (T = 300 K), n_p is the number of electrons transferred (n_p = 1 for Re$^{VI/V}$ redox couple), A is the active surface area of the electrode (A = 0.02 cm^2), D is the diffusion coefficient for the complex, [C] is the concentration of the catalyst, and ν is the scan rate. The diffusion coefficients (D) were calculated from the slopes of $i_p - \nu^{1/2}$ plots. Therefore, For Complex **1**, D = $\mathbf{5.82 \times 10^{-5}}$cm^2 s^{-1} and for Complex **2**, D = $\mathbf{9.85 \times 10^{-5}}$ cm^2 s^{-1} .
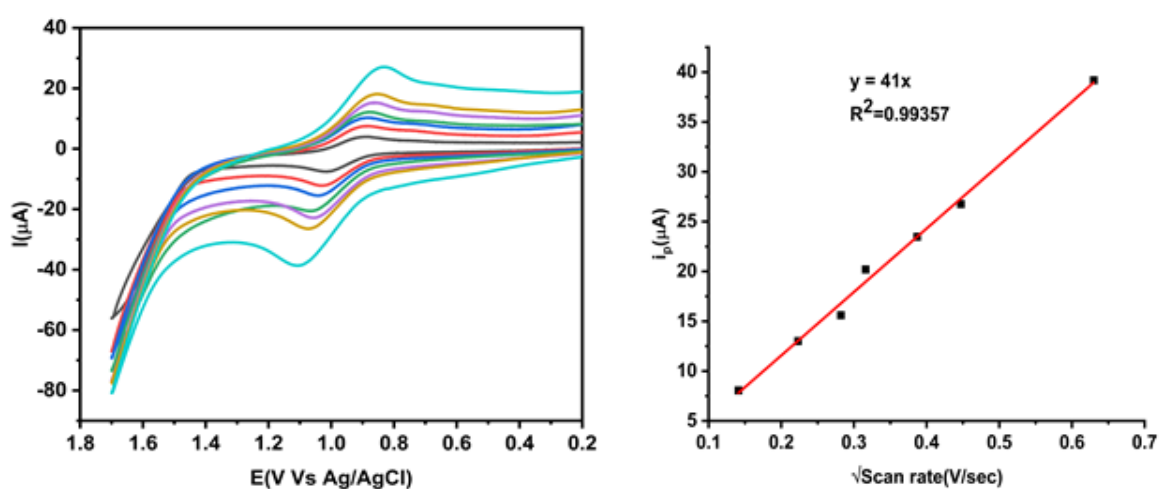
Figure S11. a) Current *vs.* potential plot in different scan rate and b) Ip vs. $\nu^{1/2}$ plot Complex **1**

(a)   (b)
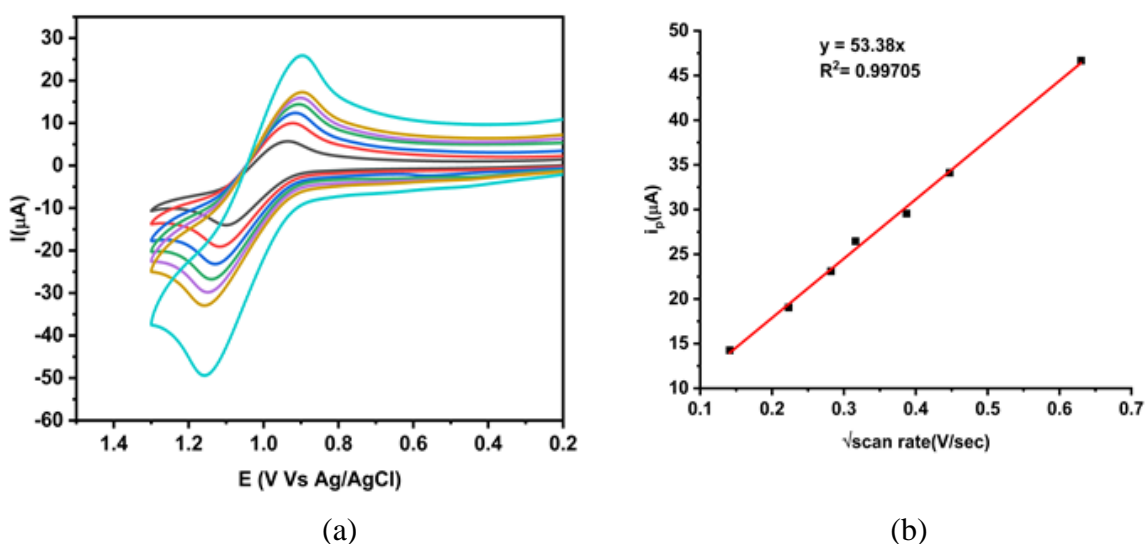
Figure S12. a) Current *vs.* potential plot in different scan rate and b)Ip vs. $\nu^{1/2}$ plot Complex-**2**
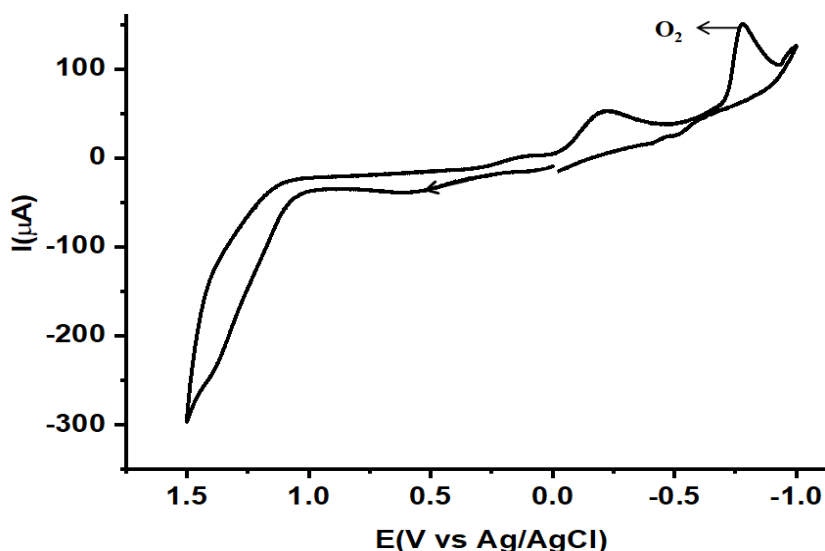
Figure S13. O_2 produced during OER (Oxygen Evolution Reaction) reduced in-situ by the working electrode at the reverse cathodic scan at argon atmosphere.

Faradaic Yield Calculation of Complex 1:

FY is determined by the equation FY (%) = 100 X 4 X amount of O_2 produced (mol)/ (Amount of charge consumed during BE/F)

During the constant potential electrolysis (working electrode Glassy carbon electrode) at 1.3 V, total charged consumed 51.1 C, gas produced= 1.97 ml. So, FY is 67 %

TOF_{max} calculations of Complex 1 from cyclic voltammetry experiments:

The turnover frequency (TOF) is an inherent characteristic of catalysts, which represents the rate of conversion reactants into products per mole of active catalyst per unit time. The TOF value for **1** was derived using the following equation below from the catalytic cyclic voltammograms recorded CH_3CN solutions in presence of 5 mM water.

$$i_{cat}/i_P = 4.484 \times (RT/F)^{1/2}(TOF_{max})^{1/2}v^{-1/2}$$

Where, i_p is peak current, i_{cat} is the catalytic current, F is Faraday's constant (F = 96500 C), R is the universal gas constant (R = 8.314 J K^{-1} mol^{-1}), T is temperature (T = 300 K) and v is the scan rate. The TOF_{max} was calculated from the slope of i_{cat}/i_p vs $v^{-1/2}$ plot. From the i_{cat}/i_p vs 1/sqrt (scan rate), we get the slope (m) = 1.04.

Therefore, $1.04 = 4.484 \times (RT/F)^{1/2}(TOF_{max})^{1/2}$

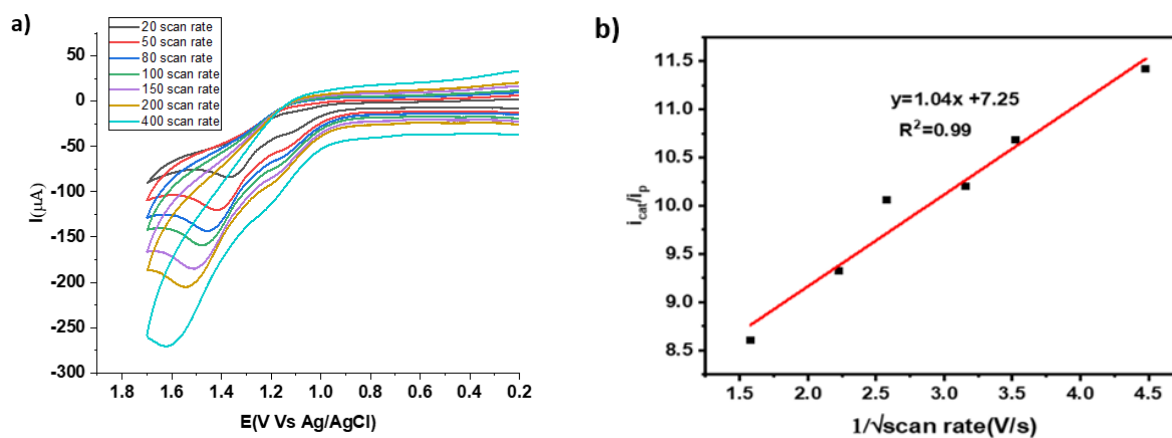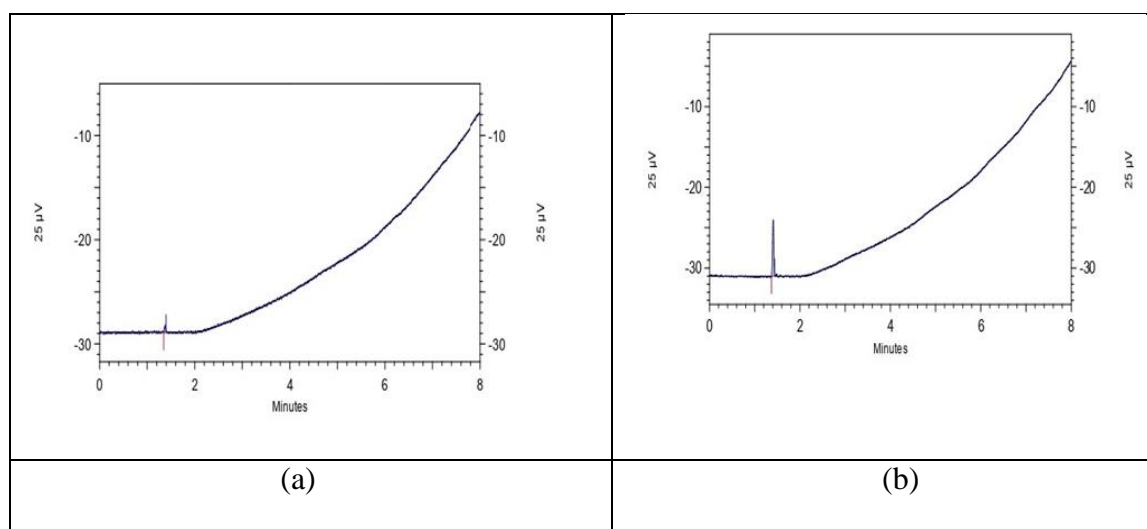$$TOF_{max} = (1.04)^2 \times 96500/(4.484^2 \times 8.314 \times 298) = 2.1 \text{ s}^{-1}$$

Figure S14. Calculation of TOF_{max} for Complex **1: a)** current vs potential plot at different scan rate **b)** i_{cat}/i_p *vs* $\nu^{-1/2}$ plot

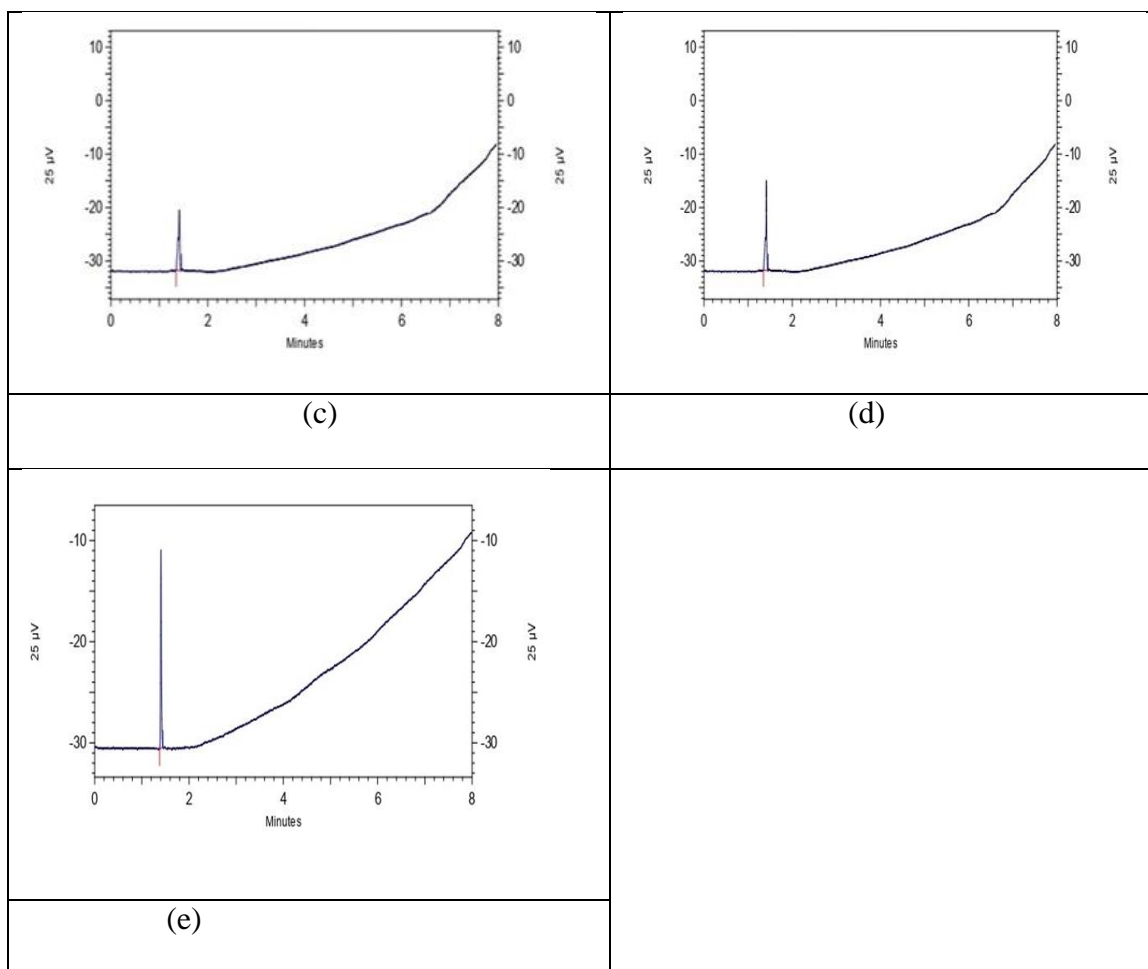**GC-TCD graph for oxygen detection over time values from CPE data:**

| (a) | (b) |

(c)

(d)

(e)

Figure S15. GC-TCD graph for oxygen detection over time. (a) 0 min. (b) 15 min. (c) 30 min. (d) 45 min. (e) 60 min. after bulk electrolysis respectively.

Amount of Oxygen determination by GC-chromatogram (Headspace analysis) and calculation of TON AND TOF.

Back Signal
Results

Retention Time	Area	Area %	Height	Height %
1.377	7935	100.00	4956	100.00

Totals	Area	Area %	Height	Height %
	7935	100.00	4956	100.00

Back Signal
Results

Retention Time	Area	Area %	Height	Height %
1.407	201233	100.00	150293	100.00

Totals	Area	Area %	Height	Height %
	201233	100.00	150293	100.00

Before bulk electrolysis the curve area of oxygen is 7935 after 60 minutes the area becomes 201233. By calibrating the GC with standard oxygen, the amount of oxygen has been calculated over time.

5 ml solution containing compound 1 (0.1 mM) and CH3CN:H2O (10:1, v/v) is used for bulk electrolysis.

The amount of O2 after 60 min of bulk electrolysis is 7.3 ml mole.

Ton =1738

Tof = 0.482 sec^{-1}
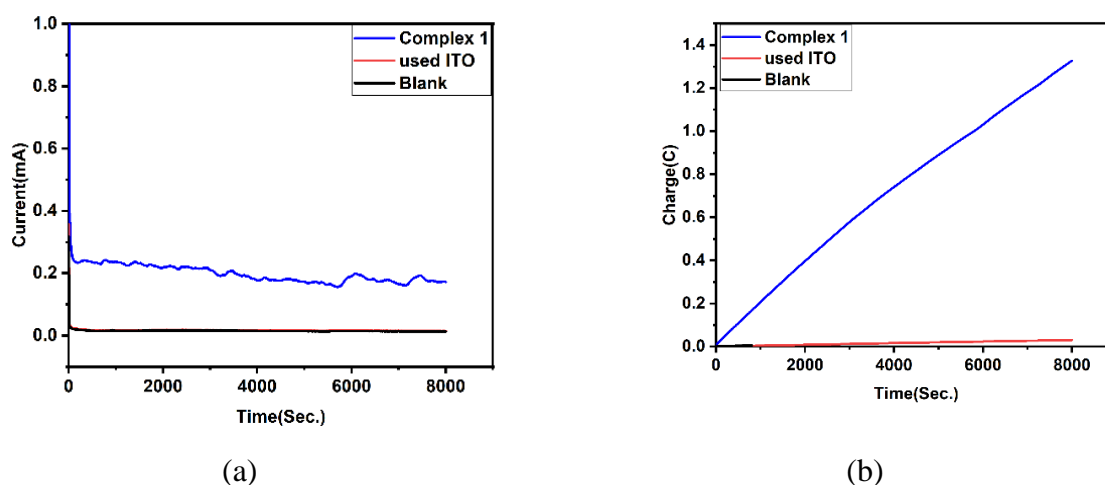
I–t curves and charge buildup during CPE.

(a)   (b)

Fig. 16 (a) charge buildup during CPE (b) I–t curves of the solution using ITO as the working electrode at 1.3 V. Black line for the 5ml solution containing CH3CN:H2O (10:1, v/v) and the complex 1(0.1mM). Red line for the used ITO electrode and blue line for the blank solution.
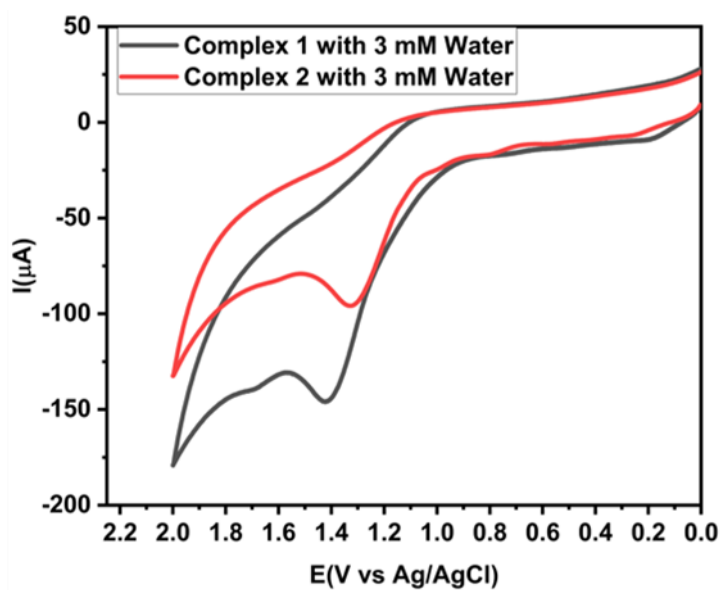
Figure S17. Current *vs.* potential plot for comparison of catalytic water oxidation by complex **1** and complex **2**

Table S1: X-ray crystallographic data of complex **1**

	Complex 1
Formula	$C_{38}H_{74}N_2O_6Cl_6Re_2$
Molecular weight	1240.11
Crystal system	monoclinic
Space group	P 21/n
a/ Å	10.488(3)
b/ Å	13.127(13)
c/ Å	17.843(6)
α/°	90
β/°	91.283(18)
γ/°	90
V/ Å^3	2456(3)
Z	2
D_{calcd} /g cm^{-3}	1.677
μ/mm^{-1}	5.292
2θ/°	3.86 to 54.32
T/K	296
R^1, wR^2 [I>2σ(I)]	R$_1$ = 0.0335, wR$_2$ = 0.0767
GOF on F^2	1.078

Table S2: Experimental and theoretical bond lengths of complex **1** and theoretical bond lengths of **1$^+$** and **1$^-$**

Experimental Bond Lengths (Å)		Calculated bond lengths(Å)		
		1	**1$^+$**	**1$^-$**
C1-C2	1.490(8)	1.508	1.494	1.451
C2-C3	1.381(8)	1.401	1.393	1.409
C3-C4	1.395(7)	1.387	1.390	1.391
C4-C5	1.490(8)	1.508	1.494	1.451
C5-C6	1.381(8)	1.401	1.393	1.409
C6-C1	1.395(7)	1.387	1.390	1.391
C1-O1	1.281(7)	1.275	1.276	1.348
C2-O2	1.273(7)	1.267	1.280	1.328
C5-O3	1.273(7)	1.267	1.280	1.328
C4-O4	1.281(7)	1.275	1.276	1.348
Re1-O5	1.682(4)	1.676	1.676	1.716
Re2-O6	1.682(4)	1.676	1.676	1.716
Re1-Cl1	2.3659(15)	2.431	2.388	2.524
Re1-Cl2	2.2989(15)	2.370	2.327	2.465
Re1-Cl3	2.3425(15)	2.431	2.388	2.524
Re2-Cl4	2.3425(15)	2.431	2.388	2.524
Re2-Cl5	2.3659(15)	2.431	2.388	2.524
Re2-Cl6	2.2989(15)	2.370	2.327	2.465
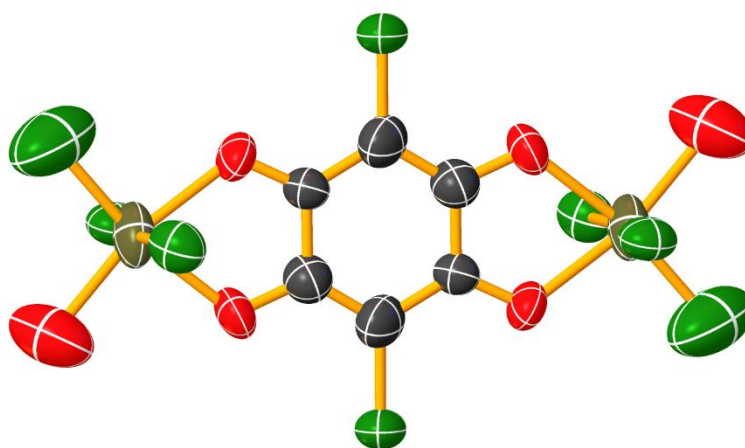
Figure S18. Molecular geometries of **2** in the crystal state (40% thermal ellipsoids, NBu$_4$ moiety omitted for clarity).

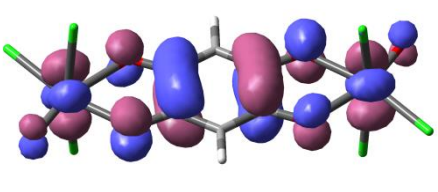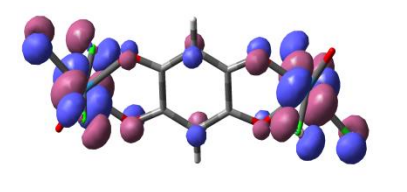**Table S3**. Isodensity plot of the selected orbital and Spin density plot of the excited states for Complex **1**
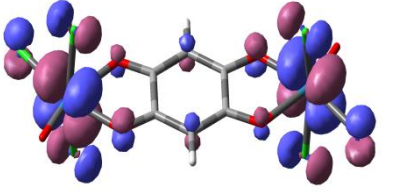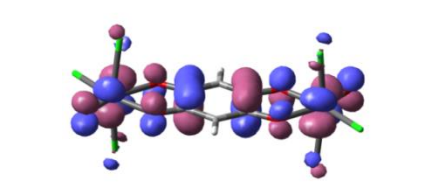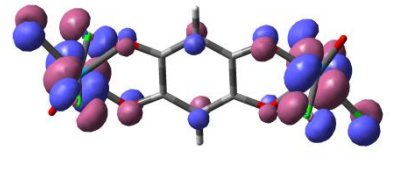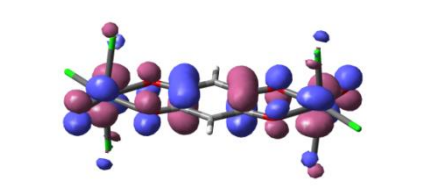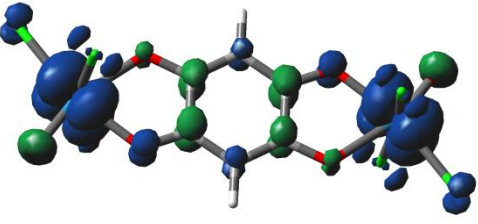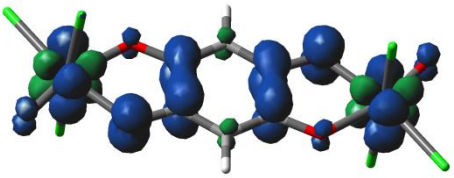
Complex 1	HOMO/LSOMO	LUMO/HSOMO
Optimised Ground state		
Optimised Excited state (Oxidised)		
Optimised Excited state (Reduced)		
Spin density (Oxidised)		
Spin density (Reduced)		

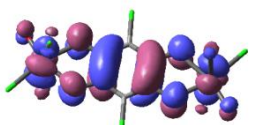**Table S4.** Isodensity plot of the selected orbital and Spin density plot of the excited states for Complex **2**
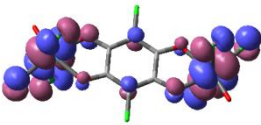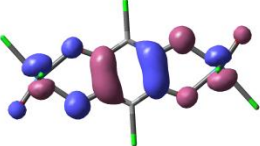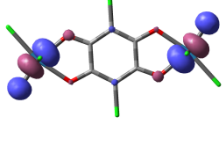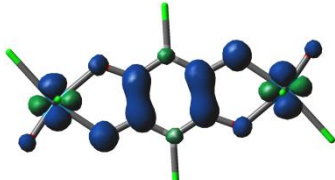
Complex 2	HOMO/LSOMO	LUMO/HSOMO
Optimised Ground state		
Optimised Excited state (Oxidised)		
Optimised Excited state (Reduced)		
Spin density (Oxidised)		
Spin density (Reduced)		

Table S5: Main calculated optical transition for the complex **1** with composition in terms of molecular orbital contribution of the transition, vertical excitation energies (λ/nm), and oscillator strength in acetonitrile.

Complex	Transition	Experimental λ_{max}/nm	Calculated λ_{max}/nm (osc.strength)	Major contributions	Assigned major Transitions
1	$S_0 \rightarrow S_1$	980	950.30(nm) (0.053)	HOMO->LUMO (47%) H-1->L+1(29%) HOMO->L+4 (22%)	$d_{xz}(Re) \rightarrow \pi^*(lig)$ dxz(Re) $\rightarrow$ dyz(Re) dxz(Re) $\rightarrow$ dxy(Re)
	$S_0 \rightarrow S_6$	640	617.72(nm) (0.3509)	HOMO>LUMO (49%), HOMO->L+4 (34%)	$d_{xz}(Re) \rightarrow \pi^*(lig)$ dxz(Re)$\rightarrow$dxy(Re)
	$S_0 \rightarrow S_{20}$	360 nm	372.97 nm (0.1885)	H-5->LUMO (76%)	dyz$\rightarrow \pi^*(lig)$

References

1   SMART SAINT, SADABS, XPREP, SHELXTL, Bruker AXS Inc., Madison, WI, 1998.

2   G.M. Sheldrick, SHELXTL, v. 6.14, Bruker AXS Inc., Madison, WI, 2003.

3   C.K. Johnson, ORTEP Report ORNL-5138, Oak Ridge National Laboratory, Oak Ridge, TN, 1976.

4   C. Lee, W.Yang, and R. G. Parr, Condens. *Matter Mater. Phys*., 1988, **37**, 785-789.

5   (a) M.E. Casida, C. Jamoroski, K.C. Casida, D.R. Salahub, *J. Chem. Phys.,* 1998, **108**, 4439-4449.

(b) R.E. Stratmann, G.E. Scuseria, M.J. Frisch, *J. Chem. Phys*., 1998,**109**, 8218-8224.

6   M.J. Frisch, G.W. Trucks, H.B. Schlegel, G.E. Scuseria, M.A. Robb, J.R. Cheeseman, G. Scalmani, V. Barone, B. Mennucci, G.A. Petersson, H. Nakatsuji, M. Caricato, X. Li, H.P. Hratchian, A.F. Izmaylov, J. Bloino, G. Zheng, J.L. Sonnenberg, M. Hada, M. Ehara, K. Toyota, R. Fukuda, J. Hasegawa, M. Ishida, T.

Nakajima, Y. Honda, O. Kitao, H. Nakai, T. Vreven, J.A. Montgomery Jr., J.E. Peralta, F. Ogliaro, M. Bearpark, J.J. Heyd, E. Brothers, K.N. Kudin, V.N. Staroverov, R. Kobayashi, J. Normand, K. Raghavachari, A. Rendell, J.C. Burant, S.S. Iyengar, J. Tomasi, M. Cossi, N. Rega, J.M. Millam, M. Klene, J.E. Knox, J.B. Cross, V. Bakken, C. Adamo, J. Jaramillo, R. Gomperts, R.E. Stratmann, O. Yazyev, A.J. Austin, R. Cammi, C. Pomelli, J.W. Ochterski, R.L. Martin, K. Morokuma, V.G. Zakrzewski, G.A. Voth, P. Salvador, J.J. Dannenberg, S. Dapprich, A.D. Daniels, O. Farkas, J.B. Foresman, J.V. Ortiz, J. Cioslowski, D.J. Fox, *Gaussian 09, (Revision A.1), Gaussian, Inc.,* Wallingford, CT, 2009.

7   N.M. O'Boyle, A.L. Tenderholt, K.M. Langner, *J. Comput. Chem.,* 2008, **29**,,839–845.